Title

Load Flexibility of a Residential Multi-Function Heat Pump Using Dynamic Pricing

Authors

Green, Chirsty

Chakraborty, Subhrajit

Vernon, David

Publication Date

2024-01-24

Data Availability

The data associated with this publication are available upon request.

Peer reviewed

Load Flexibility of a Residential Multi-Function Heat Pump Using Dynamic Pricing

Christy Green, PhD
Member ASHRAE

Subhrajit Chakraborty, PE
Student Member ASHRAE

David Vernon, PhD
Member ASHRAE

ABSTRACT HEADING

The increase in extreme weather conditions and greater penetration of intermittent renewable energy, such as solar and wind, have resulted in electric grid balancing challenges, and greenhouse gas emissions remain high during peak hours. Residential load flexibility programs help mitigate these challenges by shaping the electricity demand of major appliances to better match grid-level renewable electricity generation profiles. This study evaluates the load flexibility of a multi-function heat pump (MFHP) system responding to a dynamic price signal. The residential MFHP uses a single air-source heat pump outdoor unit to efficiently meet both water heating and space conditioning needs. The MFHP does not require electric resistance heaters for emergency heat or defrost, potentially avoiding the need for electrical panel upgrades commonly required when replacing gas appliances. A 14 kW (48 kBtu/h) MFHP system is installed in an occupied residential building in California. To achieve load flexibility, a rule-based control algorithm adjusts water heating and space cooling setpoints with the objective of minimizing electric energy cost in response to the dynamic price signal. Model-based control approaches require training data and forecasting, increasing the complexity and commissioning time. The simplicity of this rule-based control approach will be easier to adopt for widescale use because it has lower computational complexity, works with equipment from different manufacturers, and does not require in-depth programming and commissioning. The dynamic price signal used by the algorithm consists of a forecast of hourly prices for the next 24-hour period. The rule-based algorithm determines hourly setpoint schedules for the next 24-hour period based on the dynamic price signal for the water heating and space conditioning and communicates them to the MFHP thermostats.

INTRODUCTION

Building decarbonization, required to tackle the worth impacts of climate change, relies on widespread adoption of heat pumps (HP) for space and water heating which use electricity instead of burning fossil fuels. However, with heavy penetration of renewables, the future of the electric grid is dynamic and an increase in electrical demand from HP adoption will add to this challenge. Renewable energy sources have inherent fluctuations; for instance, solar power generation peaks around noon but becomes negligible at night. Additionally, their performance is contingent upon varying climate conditions and fluctuates from day to day. Utilities are becoming interested in dynamic retail pricing, which reflects the wholesale market and/or grid conditions (Gerke et al., 2022). Among building equipment, HP combined with energy storage capabilities can help shift peak energy demand and improve overall energy efficiency. There is a need for building energy management and load flexibility

Christy Green is a Research and Development Engineer at the UC Davis Western Cooling Efficiency Center, Davis, California. **Subhrajit Chakraborty** is a Ph.D. student in Energy Systems at UC Davis and a research engineer at the Western Cooling Efficiency Center, Davis California. **Davd Vernon** is co-director of engineering at the UC Davis Energy and Efficiency Institute, Davis, California.

controls that can respond to these dynamic utility prices while adequately meeting the space conditioning and water heating loads.

Load flexibility has been thoroughly studied and demonstrated with heat pump water heaters (HPWH) which are usually integrated with a domestic hot water (DHW) tank that is used as thermal energy storage (TES) (Clift et al., 2023; Di Silvestre et al., 2023; Engelbrecht et al., 2021). These load shifting approaches are often model-based requiring detailed knowledge of the system, or data-driven, such as the HVAC load control approach of (Wang et al., 2023). In this study, a rule-based approach is taken, which can easily adapt to a variety of equipment types due to lacking the requirement of a predictive model of any kind.

Multi-function heat pumps (MFHP) that provide residential space heating, space cooling, and water heating are versatile and can utilize multiple sources of energy based on availability and demand to maximize efficiency (Fabrizio et al., 2014). MFHPs allows integration of DHW tank as TES along with various modes of operation making it an ideal candidate for load flexibility. Air-to-air MFHP, under investigation in this study, is a single-compressor system with integrated refrigerant circuit providing space conditioning and water heating. It is noteworthy for its suitability for straightforward installation in the majority of residential homes in the United States avoiding electric resistance strip heaters and expensive electric panel upgrades (Chakraborty et al., 2023). The air-to-air MFHP due to its integrated refrigerant circuitry has the capability to perform both space cooling and domestic hot water (DHW) heating concurrently. This simultaneous mode has been demonstrated to offer increased efficiency, as it harvests heat energy from the living space for cooling, augments it with heat generated by the compressor, and efficiently transfers this combined heat to provide useful DHW (Chakraborty et al., 2022; Cho & Min Choi, 2013). Energy modeling and simulations of a similar MFHP with grid integration have shown higher energy and cost savings with larger DWH tanks, where a rule-based controls would charge the DHW during high efficiency (higher outdoor temperatures) and low-cost periods to prepare for the peak (Shen et al., 2017). However, analysis and impacts of MFHP rule-based load flexibility in response to a dynamic price signal are open questions that this study tries to address through demonstration in a single-family home.

EQUIPMENT AND TEST SITE

The physical MFHP system (Figure 1), consists of an off-the-shelf standard split system heat pump outdoor unit, indoor direct expansion (DX) air handler, hot water tank, MFHP main control board, water heating thermostat, and HVAC thermostat. The system has five modes of operation: 1) space heating, 2) space cooling, 3) water heating, 4) simultaneous water heating and space cooling, and 5) defrost. Three of the five available system operational modes are used in this study and are described in Table 1. Notably, no electric resistance heat is used by this system, making it suitable for residential electrification of homes with lower-capacity electric panels. The water heater and HVAC thermostats are WiFi-enabled, allowing two-way

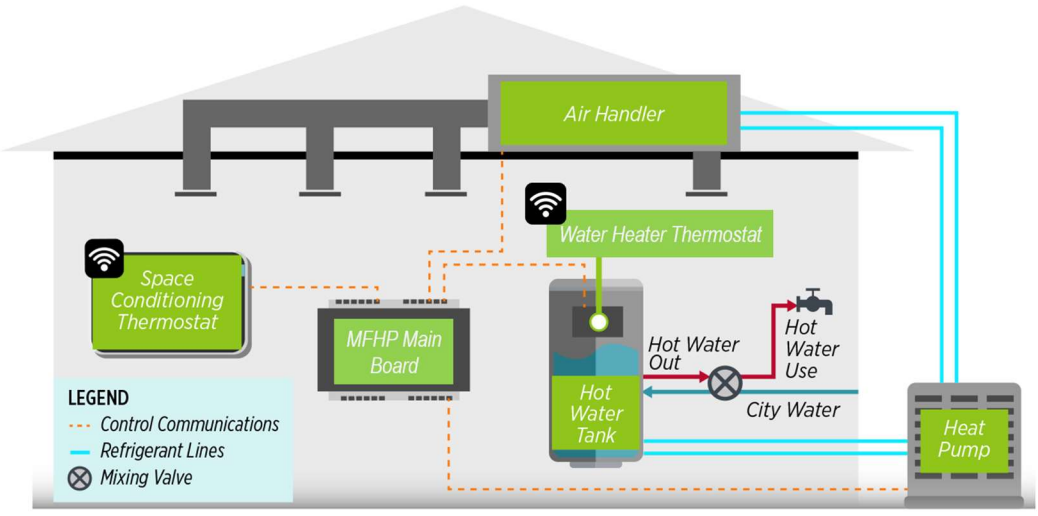

Figure 1 Multi-function integrated heat pump system configuration.

communication between the thermostats and the control algorithm hosted in the cloud. The system is installed in a 2000 ft^2 (185.8 m^2) single-family home in Davis, CA.

Table 1. Modes of Operation

Mode	Description
Water Heating	System heats water using outdoor unit
Space Cooling	System cools conditioned space using outdoor unit and air handler
Simultaneous Water Heating/Space Cooling	System simultaneously cools conditioned space and heats water, using the air handler as evaporator and water heater tank as condenser

Figure 2 presents the signal reception and communication architecture of the system. The control algorithm is hosted on a cloud server instance. No local controllers, other than those required for baseline system operation, are required, as control is achieved by adjusting the setpoints via the water heater and HVAC thermostat APIs. The dynamic price signal is received via an API request made to the Lawrence Berkeley National Laboratory (LBNL) CalFlexHub (CFH) server daily. For summer, the CFH Summer HDP price signal was used for water heating and air conditioning (HVAC) load flexibility. Once the price signal is received, the control algorithm (see Load Shifting Algorithm section) translates the signal into setpoint schedules for both the water heater and HVAC system. These setpoints are pushed to the thermostats for implementation. The hot water temperature, indoor air temperature, and setpoints are logged to ensure reliable implementation of the setpoints and detect any manual overrides by the occupants.

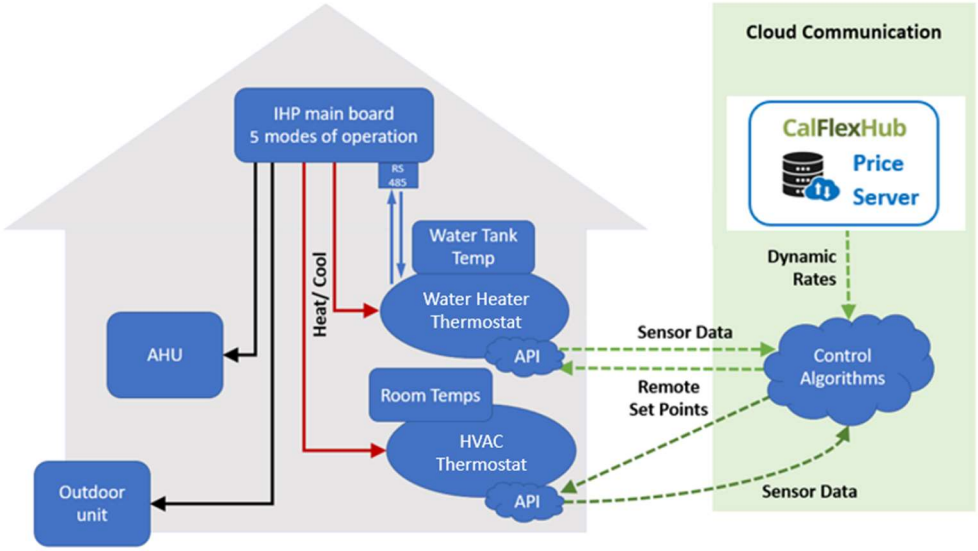

Figure 2 Signal reception and communication architecture.

LOAD SHIFTING ALGORITHM

Load shifting is achieved using a rule-based control algorithm that selects water heating and space conditioning setpoints in response to a 24-hour price signal received daily from the LBNL CFH server. The algorithm determines hourly setpoints by calculating a z-score for each hourly price over a 24-hour period (Carew et al., 2018).

$$Z(t) = \frac{p(t)-\bar{p}}{\sigma_p} \quad (1)$$

Where $p(t)$ is the price during the hour, $\bar{p}$ is the average price over the 24-hour period, and σ_p is the standard deviation of

prices over the 24-hour period. The z-scores are then scaled by multiplying by the ratio of maximum to minimum prices and a load shifting severity factor, α, and translated by a setpoint bias factor, β (Eq. 2). The value of β is assigned as zero for the preliminary tests presented.

$$Z_a(t) = Z(t)\left(\frac{\max(p)}{\min(p)}\right)\alpha + \beta \tag{2}$$

The adjusted z-scores are binned into five thresholds and associated with thermostat setpoints for water heating and space cooling functions of the MFHP, according to Eq. 3. The setpoint range and base setpoint for space cooling are determined by the occupant and the five incremental setpoints are determined by dividing this range equally. In this study, the occupant chose an upper bound of 75°F (23.9°C), mid (base) of 73°F (22.8°C), and lower bound of 70°F (21.1°C), resulting in the five values [70, 71.5, 73, 74, 75]. Occupants are not consulted on the water heater setpoints; however, they may be adjusted as needed. The five possible water heater setpoints during load shifting are [100,110,120,130,140]. The homeowner requested that the water heater never drop below 115°F (46.1°C); therefore, setpoints lower than 115°F were overridden with 115°F as encountered.

$$SP(t)\begin{cases} Z_a(t) < -1.5, & SP_1 \\ -1.5 \le Z_a(t) < -0.5, & SP_2 \\ -0.5 \le Z_a(t) < 0.5 & SP_3 \\ 0.5 \le Z_a(t) < 1.5 & SP_4 \\ 1.5 \le Z_a(t) & SP_5 \end{cases} \tag{3}$$

The lower-cost region of the price signal often causes the "load up" control action, during which the water heater is preheated and the conditioned space is precooled, to last for several hours, which is unnecessarily energy intensive. To conserve energy, only the last hour of the load up period was used and all hours preceding were lowered to the middle, or "base", setpoint, to reduce the energy used during load-up while ensuring the system is prepared for the load shed period. The resulting setpoints developed in response to the summer price signal are presented in Figure 3.

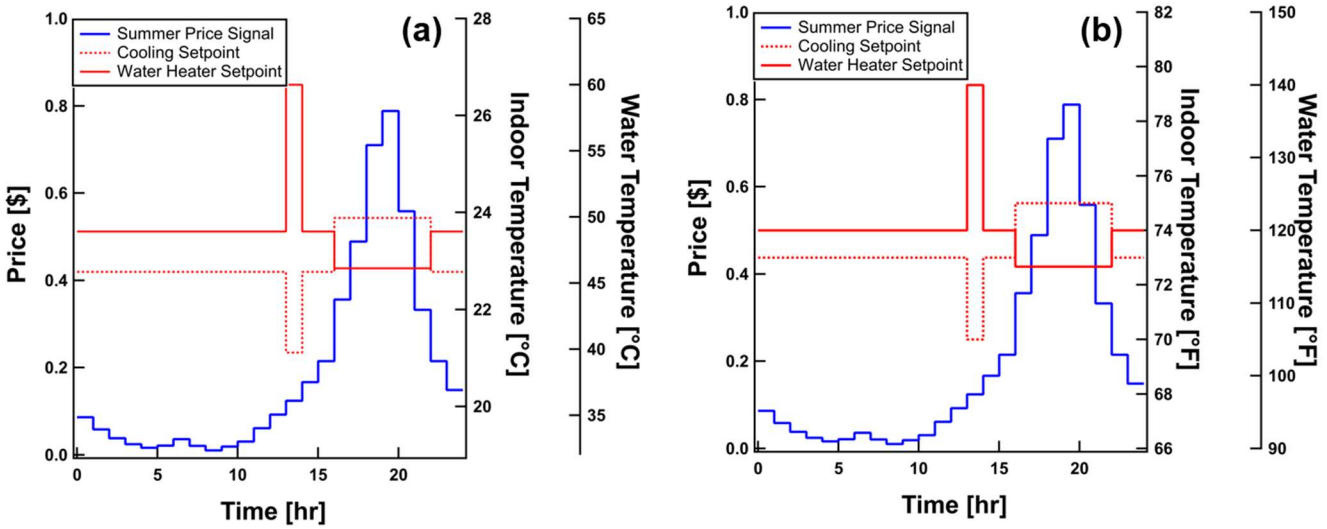

Figure 3 Water heater and HVAC thermostat setpoints ((a) SI units, (b) IP units) with corresponding summer price signal.

Additionally, a feature was added to the algorithm to force the system into simultaneous space cooling and water heating mode any time there is a call for water heating. When operating in simultaneous space cooling/water heating mode, the system achieves approximately 36% greater efficiency than operating in separate water heating and separate space cooling mode cycles (Chakraborty et al., 2023). More frequent simultaneous mode operation was achieved by decreasing the current space cooling setpoint by 2°F when a call from the water heater thermostat to the MFHP board is detected. The decreased cooling setpoint remains in effect for 30 minutes and then reverts to the scheduled cooling setpoint (e.g. a cooling setpoint of 72°F (22.2°C) would be decreased to 70°F (21.1°C) for 30 minutes upon a call for water heating. After 30 minutes, the cooling setpoint would return to 72°F (22.2°C)). This allows the system to take advantage of the higher system efficiency achieved by heating water in the simultaneous mode as frequently as possible.

RESULTS

Water heating load shifting at the Davis, CA field site was performed from June 08, 2023 through July 26, 2023. This was followed by a period of water heating and HVAC space cooling load flexibility testing (July 27, 2023 – August 7, 2023), using both the water heater and HVAC components of the system. Maximum peak power and peak energy use during the 6:00 PM – 10:00 PM peak time, and daily electricity cost are used as performance metrics for load flexibility impacts. The peak demand period for summer is specified as 6:00 PM – 10:00 PM, seven days a week.

Two-Day Load Shifting Example

Two days are presented as an example of load shifting controlling both the water heating and HVAC systems (combined load shift), Figure 4. These days are presented to give a visual representation of the load shift operation and provide insight into specific system behaviors typically encountered during combined load shifting. Figure 4 presents the system performance

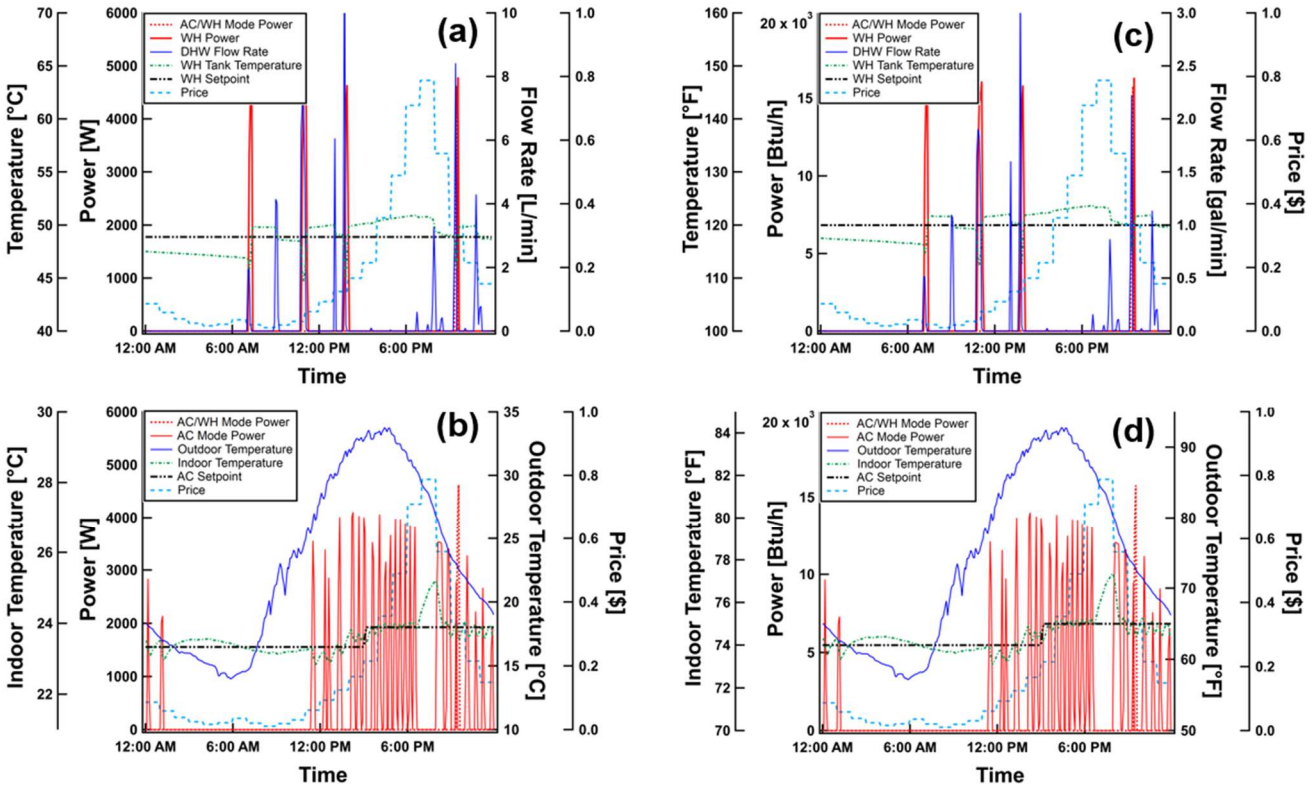

Figure 4 Baseline (a), (c) water heating and (b), (d) space cooling operation.

on the baseline day, July 25, 2022, and Figure 5 presents a load shifting day, July 28, 2023. These days were chosen by finding days with the least mean absolute error between points in the outdoor temperature and volumetric hot water flow rate time series. During the baseline day (Figure 4), the system operated frequently for shorter time periods to maintain the cooling setpoint temperature and operated in the dual water heating/space conditioning for 10 minutes, as compared to 45 minutes during the load shift day. The water heater maintained a constant 120°F (48.9°C) setpoint throughout the day, and the HVAC system maintained a user-specified programmed schedule consisting of two setpoints.

During the load shifting day (Figure 5), the simultaneous water heating/space cooling mode was triggered twice by the algorithm, increasing system efficiency. The elevated water temperature achieved prior to the peak period resulted in no electricity consumption associated with water heating during the peak. The reduced indoor air temperature leading into the peak period reduced the amount of energy required for space cooling during the peak. It may also be noted in Figure 5 that the occupants are capable of overriding the setpoint temperature if they wish. The early morning hours see a period of elevated cooling setpoint associated with a manual thermostat adjustment made by the occupant.

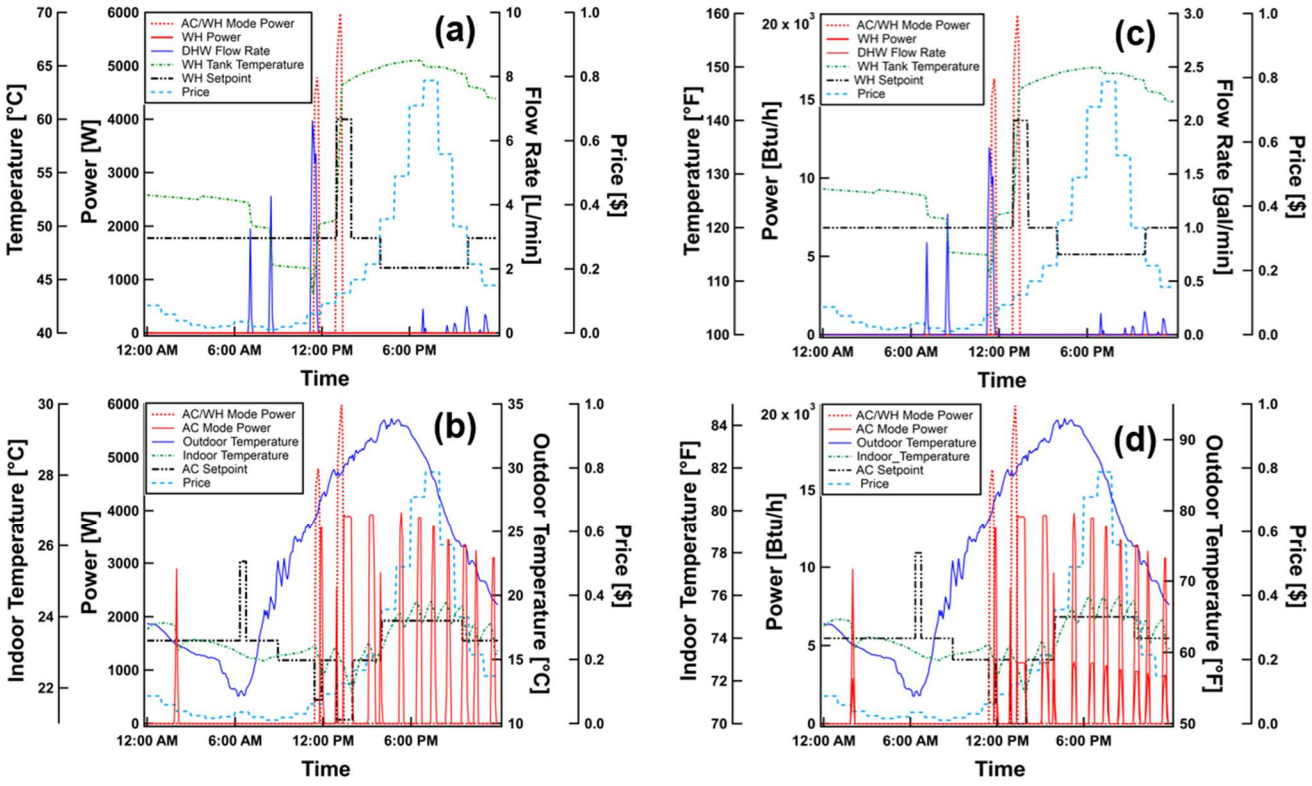

Figure 5 Combined load shifting controlling (a), (c) water heating and (b), (d) space cooling operation.

A comparison of peak power, peak energy consumption, and cost is presented in Table 2. The 17% lower peak power draw is due to the system operating only in space cooling mode over the peak period, which draws less power than both water heating and simultaneous water heating/space cooling modes. Total energy use during the peak period was reduced 39%, and overall daily cost was reduced 17%.

These results provide an example of one day of load shifting, but more days must be considered to develop a clearer idea of the load shifting potential during cooling season. In the following section, a longer period of time is analyzed for the

Table 2. Results for Combined Water Heating and HVAC Load Shifting

Metric	Baseline	Load Shift	Change [%]
Mean Daily Peak* Electric Power	4,787 W (16,334 Btu/h)	3,970 W (13,546 Btu/h)	-17%
Mean Daily Total Peak* Electrical Energy	7.96 kWh (27.16 kBtu)	4.82 kWh (16.45 kBtu)	-39%
Mean Daily Electricity Cost [$]	5.07	4.19	-17%

*Peak demand period is 6-10 PM, every day

combined water heater and HVAC load shift, along with an analysis of load shift controlling only the water heater.

Multi-Day Load Shifting Evaluation

Making day-to-day comparisons of key metrics for load shifting is difficult due to the impact of highly variable external factors like weather and water use patterns. To make a broad assessment of the load shifting performance, the mean daily value for each metric was calculated over the course of the combined (WH + HVAC) and water heater-only load shifting periods and compared to the metrics of a similar period in the prior, baseline, year. To determine a suitable baseline period, the daily cooling degree days and total daily water use by volume in the load shift and candidate baseline periods were calculated and distributions were fit to the resulting data (Figure 6). Baseline periods with similar distributions for cooling degree days (CDD) and water use were chosen for comparison. CDD distribution is important even only controlling the water heater for load shifting, due to the split-system design in which the heat pump water heater evaporator is located in the outdoor unit.

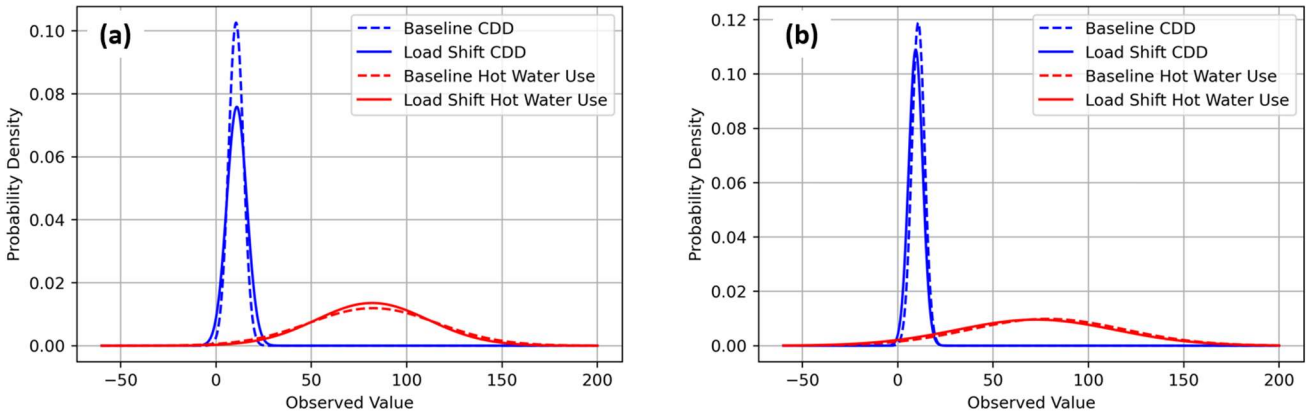

Figure 6 (a) Water heating-only and (b) combined water heating and HVAC cooling degree day and water volume (gallons) distributions for baseline and load shifting period days.

The results for the multi-day load shift evaluation controlling only water heating are presented in Table 3. The 16% decrease in daily total peak energy and 14% daily cost reduction are expected, as the load shifting algorithm shifts energy consumption to the lower-cost periods preceding and exceeding the peak period as much as possible. Because the system operational modes themselves are not altered, and the system must still occasionally operate during the peak period, the 10% reduction in maximum peak power was more unexpected. However, this may be explained by the load shift algorithm often completely removing water heating from the peak period, as the system draws more power in water heating mode than space cooling.

The results of the multi-day evaluation of combined water heating and HVAC load shifting are presented in Table 4. The trends in the results are similar to those achieved using water heating alone, although a significant reduction in total peak energy

was achieved, as compared to the water heating-only load shift.

Table 3. Multi-Day Results for Water Heating Load Shifting

Metric	Baseline (2022-06-20 – 2022-07-26)	Load Shift (2023-07-01 – 2023-07-26)	Change [%]
Mean Daily Maximum Peak* Electric Power	4,631 W (15,801 Btu/h)	4,180 W (14,263 Btu/h)	-10%
Mean Daily Total Peak* Electrical Energy	10.03 kWh (34.22 kBtu)	8.46 kWh (28.87 kBtu)	-16%
Mean Daily Electricity Cost [$]	6.70	5.77	-14%
*Peak demand period is 6-10 PM, every day			

Table 4. Multi-Day Results for Combined Water Heating and HVAC Load Shifting

Metric	Baseline (2022-07-01 – 2022-08-31)	Load Shift (2023-07-27 – 2023-08-07)	Change [%]
Mean Daily Maximum Peak* Electric Power	4,490 W (15,320 Btu/h)	3,982 W (13,587 Btu/h)	-11%
Mean Daily Total Peak* Electrical Energy	8.96 kWh (30.57 kBtu)	6.39 kWh (21.80 kBtu)	-29%
Mean Daily Electricity Cost [$]	5.93	5.19	-12%
*Peak demand period is 6-10PM every day			

CONCLUSION

Multi-function heat pumps may provide a viable alternative to typical electric HVAC and water heating systems, while allowing electrification without an electrical panel upgrade. Along with electrification, they may be used in load flexibility programs that further facilitate the adoption of inherently variable renewable energy resources. In this study, load shifting was accomplished using both the water heating and space cooling functions of the MFHP to achieve savings in maximum peak power, total peak energy, and electricity cost. Notably, total peak energy use was lowered by 16% by controlling the water heater alone, and 29% when controlling the combined water heater and HVAC system. Maximum peak power was reduced by ~10-11%, as a result of reducing water heater operation during peak hours. Future work will focus on further increasing cost savings (currently ~12%) by investigating the effect of timing and setpoint choice on combined load shift outcomes. Other means of evaluation may also be investigated and applied to load shifting periods covering a wider range of climate conditions and occupant water use patterns from additional test sites.

ACKNOWLEDGMENTS

The authors would like to acknowledge the California Energy Commission CalFexHub program for funding, Lawrence Berkeley National Laboratory for guidance, and Villara Corporation for the development of the multi-function heat pump equipment.

NOMENCLATURE

α = load shifting severity factor
β = setpoint bias factor
p = price
σ = standard deviation
Z = z-score
Z_a = adjusted z-score

REFERENCES

Carew, N., Larson, B., Piepmeier, L., & Logsdon, M. (2018). *Heat Pump Water Heater Electric Load Shifting: A Modeling Study*. Ecotope. Inc.

Chakraborty, S., Chally, S., & Levering, T. (2023, May 15). *Enabling Electrification of Domestic Hot Water and Space Conditioning with Multi-function Heat Pumps*. IEA International Heat Pump Conference, 14, Chicago. https://escholarship.org/uc/item/1w62664v

Chakraborty, S., Mcmurry, R., & Harrington, C. (2022). *Concurrent Space Cooling and Hot water Heating through Compact Heat Pumps for All-electric Residential Buildings*. UC Davis. https://escholarship.org/uc/item/9565g85j

Cho, C., & Min Choi, J. (2013). Experimental investigation of a multi-function heat pump under various operating modes. *AFORE 2011(Asia-Pacific Forum of Renewable Energy 2011)*, *54*, 253–258. https://doi.org/10.1016/j.renene.2012.07.017

Clift, D. H., Stanley, C., Hasan, K. N., & Rosengarten, G. (2023). Assessment of advanced demand response value streams for water heaters in renewable-rich electricity markets. *Energy*, *267*, 126577. https://doi.org/10.1016/j.energy.2022.126577

Di Silvestre, M. L., Riva Sanseverino, E., Telaretti, E., & Zizzo, G. (2023). Flexibility of grid interactive water heaters: The situation in the US. *Renewable and Sustainable Energy Reviews*, *182*, 113425. https://doi.org/10.1016/j.rser.2023.113425

Engelbrecht, J. A. A., Ritchie, M. J., & Booysen, M. J. (2021). Optimal schedule and temperature control of stratified water heaters. *Energy for Sustainable Development*, *62*, 67–81. https://doi.org/10.1016/j.esd.2021.03.009

Fabrizio, E., Seguro, F., & Filippi, M. (2014). Integrated HVAC and DHW production systems for Zero Energy Buildings. *Renewable and Sustainable Energy Reviews*, *40*, 515–541. https://doi.org/10.1016/j.rser.2014.07.193

Gerke, B., Stübs, M., Murthy, S., Khandekar, A., Cappers, P., Brown, R., & Piette, M. A. (2022). *Potential bill impacts of dynamic electricity pricing on California utility customers*. Lawrence Berkeley National Laboratory.

Shen, B., New, J., & Baxter, V. (2017). Air source integrated heat pump simulation model for EnergyPlus. *Energy and Buildings*, *156*, 197–206. https://doi.org/10.1016/j.enbuild.2017.09.064

Wang, H., Chen, Y., Kang, J., Ding, Z., & Zhu, H. (2023). An XGBoost-Based predictive control strategy for HVAC systems in providing day-ahead demand response. *Building and Environment*, *238*, 110350. https://doi.org/10.1016/j.buildenv.2023.110350